Vacuum structure of spontaneously broken $\mathcal{N} = 2$ supersymmetric gauge theory

Masato Arai [a] [*] and Nobuchika Okada [b] [†]

[a]*Department of Physics, Tokyo Metropolitan University,*
Hachioji, Tokyo 192-0397, Japan
[b]*Theory Group, KEK, Tsukuba, Ibaraki 305-0801, Japan*

Abstract

We analyze the vacuum structure of spontaneously broken $\mathcal{N} = 2$ supersymmetric gauge theory with the Fayet-Iliopoulos term. Our theory is based on the gauge group $SU(2) \times U(1)$ with $N_f = 1, 2$ massless quark hypermultiplets having the same $U(1)$ charges. In the classical potential, there are degenerate vacua even in the absence of supersymmetry. It is shown that this vacuum degeneracy is smoothed out, once quantum corrections are taken into account. In $N_f = 1$ case, the effective potential is found to be so-called runaway type, and there is neither well-defined vacuum nor local minimum. On the other hand, in $N_f = 2$ case, while there is also the runaway direction in the effective potential, we find the possibility that there appears the local minimum with broken supersymmetry at the degenerate dyon point.

[*]e-mail: m-arai@phys.metro-u.ac.jp

[†]e-mail: okadan@camry.kek.jp

I. INTRODUCTION

There has been much progress in understanding the dynamics of strongly coupled $\mathcal{N} = 1, 2$ supersymmetric (SUSY) gauge theories. The exact effective superpotential can be derived for $\mathcal{N} = 1$ SUSY QCD (SQCD) by using holomorphy properties of the superpotential and the gauge kinetic function [1]. Seiberg and Witten derived the exact low energy Wilsonian effective action for $\mathcal{N} = 2$ SUSY $SU(2)$ Yang-Mills theory [2], and generalized their discussion to the case with up to four massive quark hypermultiplets [3]. The key ingredients which allow us to derive the exact results are duality and holomorphy. One can write down the prepotential and the gauge couplings in terms of the meromorphic differential on the Riemann surface with genus one whose properties are determined by the dynamical scale and the hypermultiplet masses.

The results by Seiberg and Witten were extended to the case with the explicit soft SUSY breaking terms by using the spurion technique. Unless these terms do not change the holomorphy and duality properties of the theory, we can derive the exact effective action for $\mathcal{N} = 1$ and $\mathcal{N} = 0$ (non-supersymmetric) SUSY gauge theories up to the leading order for the soft SUSY breaking terms. In Refs. [4,5], the exact superpotential and the phase structure in $\mathcal{N} = 1$ SQCD were discussed based on the $\mathcal{N} = 2$ SUSY gauge theory with some soft breaking terms. In Refs. [6–8], the vacuum structure of non-SUSY gauge theory was investigated in which soft SUSY breaking terms directly break $\mathcal{N} = 2$ SUSY to $\mathcal{N}=0$. As further extensions, the method to introduce non-holomorphic soft SUSY breaking terms was recently discussed [9].

In this paper, we study a spontaneously broken $\mathcal{N} = 2$ SUSY gauge theory. It is well known that, in the framework of $\mathcal{N} = 2$ SUSY theory, the only possibility to break SUSY spontaneously is to introduce the Fayet-Iliopoulos (FI) term [10]. Therefore, in the following, we consider the gauge theory which includes $U(1)$ gauge interaction together with the FI term.

The simplest example of this type of theory is $\mathcal{N} = 2$ SUSY QED (SQED) with the FI term [11]. At the classical level, although SUSY is spontaneously broken in Coulomb branch, there are degenerate vacua (moduli space) which are parameterized by the vacuum expectation value of the scalar field, a, in the $U(1)$ vectormultiplet. The direction of this vacuum degeneracy in the absence of SUSY is called "pseudo flat" direction. However, it is expected that this direction is lifted up, once quantum corrections are taken into account. By virtue of $\mathcal{N} = 2$ SUSY, the effective action is found to be one loop exact, and the effective gauge coupling is given by $e(a)^2 \sim 1/\log(\Lambda_L/a)$, where Λ_L is the Landau pole. Note that there are two singular regions in moduli space, namely, the ultraviolet region such as $|a| \geq \Lambda_L$, and the massless singular point at the origin $a = 0$. Since the effective potential is described as $V \sim e(a)^2$, the potential minimum emerges at the origin, where SUSY is formally restored. However, since this point is the singular point, we conclude that there is no well-defined vacuum in this theory.

In this paper, we investigate the vacuum structure of more interesting theory with spontaneous $\mathcal{N} = 2$ SUSY breaking. Our theory is based on the gauge group $SU(2) \times U(1)$ with $N_f = 1, 2$ massless quark hypermultiplets having the same $U(1)$ charges. In the ultraviolet region, the behavior of the effective potential can be well understood based on the perturbative discussion, since the $SU(2)$ gauge interaction is weak there. On the other hand, it

is expected that the behavior of the effective potential in the infrared region is drastically changed compared with SQED, because of the presence of the $SU(2)$ gauge dynamics.

The paper is organized as follows. In the next section, we briefly discuss the classical structure of our theory. It is shown that the classical potential has the pseudo flat direction. In Sec. III, the low energy effective action is discussed. In the subsection A, we first make our framework clear, and give general formulae of the effective action. The effective potential can be read off from this effective action, and is explicitly presented in the subsection B. In the subsection C, we give the explicit formulae for the periods and the effective gauge couplings which are necessary to analyze the effective potential. In Sec. IV, the effective potential is numerically analyzed, and the vacuum structures of our theory are investigated for both cases of $N_f = 1$ (subsection A) and $N_f = 2$ (subsection B). In Sec. V, we give our conclusions. Some formulae and technical details used in our analysis are summarized in Appendices A and B.

II. CLASSICAL STRUCTURE OF $\mathcal{N} = 2$ $SU(2) \times U(1)$ GAUGE THEORY

In this section, we briefly discuss the classical structure of our theory. The complete analysis of the classical potential was originally addressed in Ref. [10].

We describe the classical Lagrangian in terms of $\mathcal{N} = 1$ superfields: adjoint chiral superfield A_i, superfield strength W_i and vector superfield V_i in the vectormultiplet ($i = 1, 2$ denote the index of the $U(1)$ and the $SU(2)$ gauge symmetries, respectively), and two chiral superfields Q^i_α and $\tilde{Q}^\alpha_i$ in the hypermultiplet ($i = 1, ..., N_f$ is the flavor index, and $\alpha = 1, 2$ is the $SU(2)$ color index). The classical Lagrangian is given by

$$\mathcal{L} = \mathcal{L}_{HM} + \mathcal{L}_{VM} + \mathcal{L}_{FI} , \tag{1}$$

$$\mathcal{L}_{HM} = \int d^4\theta \left(Q^\dagger_i e^{2V_2 + 2V_1} Q^i + \tilde{Q}_i e^{-2V_2 - 2V_1} \tilde{Q}^{\dagger i} \right)$$
$$+ \sqrt{2} \left(\int d^2\theta \tilde{Q}_i \left(A_2 + A_1 \right) Q^i + h.c. \right) , \tag{2}$$

$$\mathcal{L}_{VM} = \frac{1}{2\pi} \mathrm{Im} \left[\mathrm{tr} \left\{ \tau_{22} \left(\int d^4\theta A^\dagger_2 e^{2V_2} A_2 e^{-2V_2} + \frac{1}{2} \int d^2\theta W^2_2 \right) \right\} \right]$$
$$+ \frac{1}{4\pi} \mathrm{Im} \left[\tau_{11} \left(\int d^4\theta A^\dagger_1 A_1 + \frac{1}{2} \int d^2\theta W^2_1 \right) \right] , \tag{3}$$

$$\mathcal{L}_{FI} = \int d^4\theta \xi V_1 , \tag{4}$$

where $\tau_{22} = i\frac{4\pi}{g^2} + \frac{\theta}{2\pi}$ and $\tau_{11} = i\frac{4\pi}{e^2}$ are the gauge couplings of the $SU(2)$ and the $U(1)$ gauge interactions, respectively. Here we take the notation, $T(R)\delta^{ab} = \mathrm{tr}(T^a T^b) = \frac{1}{2}\delta^{ab}$. The same $U(1)$ charge of the hypermultiplets is normalized to be one. The last term in Eq. (1) is the FI term with the coefficient ξ of mass dimension two.

From the above Lagrangian, the classical potential is read off as

$$V = \frac{1}{g^2} \mathrm{tr}[A_2, A^\dagger_2]^2 + \frac{g^2}{2} (q^\dagger_i T^a q^i - \tilde{q}_i T^a \tilde{q}^{\dagger i})^2$$
$$+ q^\dagger_i [A_2, A^\dagger_2] q^i - \tilde{q}_i [A_2, A^\dagger_2] \tilde{q}^{\dagger i} + 2g^2 |\tilde{q}_i T^a q^i|^2$$

3

$$+ \frac{e^2}{2} \left(\xi + q_i^\dagger q^i - \tilde{q}_i \tilde{q}^{\dagger i} \right)^2 + 2e^2 |\tilde{q}_i q^i|^2$$
$$+ 2 \left(q_i^\dagger |A_2 + A_1|^2 q^i + \tilde{q}_i |A_2 + A_1|^2 \tilde{q}^{\dagger i} \right) , \tag{5}$$

where A_2, A_1, q^i and $\tilde{q}_i$ are scalar components of the corresponding chiral superfields, respectively. The potential minimum is obtained by solving the stationary conditions with respect to these scalar components. There are some solutions, and one example is given by

$$q_\alpha^i = 0, \ \ \tilde{q}_1^\alpha = \delta_1^\alpha \left(\frac{e^2}{\frac{1}{4}g^2 + e^2} \xi \right)^{\frac{1}{2}}, \ \ \tilde{q}_j^\alpha = 0 \ \ (j \neq 1),$$
$$A_2 + A_1 = \begin{pmatrix} \frac{a_2}{2} & 0 \\ 0 & -\frac{a_2}{2} \end{pmatrix} + \begin{pmatrix} a_1 & 0 \\ 0 & a_1 \end{pmatrix} = \begin{pmatrix} 0 & 0 \\ 0 & z \end{pmatrix}, \tag{6}$$

where a_1 and a_2 are complex parameters, and z is arbitrary constant. In this example, the gauge symmetry $SU(2) \times U(1)$ is broken to $U(1)$. The potential energy is given by

$$V = \frac{\xi^2}{2} \frac{e^2 g^2}{4e^2 + g^2}. \tag{7}$$

Note that the classical potential has the pseudo flat direction parameterized by a_1 or a_2 with the condition $a_1 + \frac{1}{2}a_2 = 0$. We expect that this direction is lifted up, once quantum corrections are take into account, and the true non-degenerate vacuum is selected out after the effective potential is analyzed. This naive expectation seems natural, if we notice that the above potential energy is described by the bare gauge couplings, which should be replaced by the effective one (non-trivial functions of moduli parameters) in the effective theory.

III. QUANTUM STRUCTURE OF $\mathcal{N} = 2$ $SU(2) \times U(1)$ GAUGE THEORY

A. Effective Action

In this subsection, we describe the low energy Wilsonian effective Lagrangian of our theory. If we could completely integrate the action to zero momentum, the exact effective Lagrangian $\mathcal{L}_{EXACT}$ could be obtained, which is described by light fields, the dynamical scale and the coefficient of the FI term ξ. However, this is highly non-trivial and very difficult task. In the following discussion, suppose that the coefficient ξ, the order parameter of SUSY breaking, is much smaller than the dynamical scale of the $SU(2)$ gauge interaction. Then we consider the effective action up to the leading order of ξ. The exact effective Lagrangian, if it could be obtained, can be expanded with respect to the parameter ξ as

$$\mathcal{L}_{EXACT} = \mathcal{L}_{SUSY} + \xi \mathcal{L}_1 + \mathcal{O}(\xi^2). \tag{8}$$

Here, the first term $\mathcal{L}_{SUSY}$ is the exact effective Lagrangian containing full SUSY quantum corrections. The second term is the leading term of ξ, and nothing but the FI term at tree level. [1] Analyzing the effective Lagrangian up to the leading order of ξ, we obtain the

---

[1] Considering all the symmetries of our theory, we find that the FI term is tree-level exact [11].

effective potential of the order of ξ^2. The coefficient of ξ^2 in the effective potential includes full SUSY quantum corrections. Therefore, in our aim, what we need to analyze the effective potential is nothing but the effective Lagrangian $\mathcal{L}_{SUSY}$.

Except the FI term, the classical $SU(2) \times U(1)$ gauge theory has moduli space, which is parameterized by a_2 and a_1. On this moduli space except the origin, the gauge symmetry is broken to $U(1)_c \times U(1)$. Here $U(1)_c$ denotes the gauge symmetry in the Coulomb phase originated from the $SU(2)$ gauge symmetry. Before discussing the effective action of this theory, we should make it clear how to treat the $U(1)$ gauge interaction part. In the following analysis, this part is, as usual, discussed as a cut-off theory. [2] Thus, the Landau pole Λ_L is inevitably introduced in our effective theory, and the defined region of the moduli parameter a_1 is constrained within the region $|a_1| < \Lambda_L$. According to this constraint, the defined region for moduli parameter a_2 is found to be also constrained in the same region, since two moduli parameters are related with each other through the hypermultiplets. We take the scale of Λ_L to be much larger than the dynamical scale of the $SU(2)$ gauge interaction Λ_{N_f}, so that the $U(1)$ gauge interaction is always weak in the defined region of moduli space. Note that, in our framework, we implicitly assume that the $U(1)$ gauge interaction have no effect on the $SU(2)$ gauge dynamics. This assumption is justified in the following discussion about the monodromy transformation (see Eq. (12)).

We first discuss the general formulae for the effective Lagrangian $\mathcal{L}_{SUSY}$, which consists of two parts described by light vectormultiplets and hypermultiplets, $\mathcal{L}_{SUSY} = \mathcal{L}_{VM} + \mathcal{L}_{HM}$. The vectormultiplet part $\mathcal{L}_{VM}$, which is consistent with $\mathcal{N} = 2$ SUSY and all the symmetries in our theory, is given by

$$\mathcal{L}_{VM} = \frac{1}{4\pi} \text{Im} \left\{ \sum_{i,j=1}^{2} \left(\int d^4\theta \frac{\partial F}{\partial A_i} A_i^\dagger + \int d^2\theta \frac{1}{2} \tau_{ij} W_i W_j \right) \right\}, \tag{9}$$

where $F(A_2, A_1, \Lambda_{N_f}, \Lambda_L)$ is the prepotential, which is the function of moduli parameters a_2, a_1, the dynamical scale Λ_{N_f}, and the Landau pole Λ_L. The effective coupling τ_{ij} is defined as

$$\tau_{ij} = \frac{\partial^2 F}{\partial a_i \partial a_j} \quad (i, j = 1, 2). \tag{10}$$

The part $\mathcal{L}_{HM}$ is described by a light hypermultiplet with appropriate quantum number $(n_e, n_m)_n$, where n_e is electric charge, n_m is magnetic charge, and n is the $U(1)$ charge. This part should be added to the effective Lagrangian around a singular point on moduli space, since the hypermultiplet is expected to be light there and enjoys correct degrees of freedom in the effective theory. The explicit description is given by

$$\mathcal{L}_{HM} = \int d^4\theta \left(M^\dagger e^{2n_m V_{2D} + 2n_e V_2 + 2n V_1} M + \tilde{M} e^{-2n_m V_{2D} - 2n_e V_2 - 2n V_1} \tilde{M}^\dagger \right) \tag{11}$$

$$+ \sqrt{2} \left(\int d^2\theta \tilde{M} (n_m A_{2D} + n_e A_2 + n A_1) M + h.c. \right),$$

---

[2] There is a possibility that non-trivial fixed point and the strong coupling phase exist in QED [12]. This problem is very difficult, and is out of our scope (see also Ref. [11] for related discussions).

where M and $\tilde{M}$ denote light quark or light dyon hypermultiplet, that is, the light BPS state, and V_{2D} is the dual gauge field of $U(1)_c$.

In order to obtain an explicit description of the effective Lagrangian, let us consider the monodromy transformation of our theory. Suppose that moduli space is parameterized by the vectormultiplet scalars a_2, a_1 and their duals a_{2D}, a_{1D} which are defined as $a_{iD} = \partial F/\partial a_i$ $(i = 1, 2)$. These variables are transformed into their linear combinations by the monodromy transformation. In our case, the monodromy transformation is subgroup of $Sp(4, \mathbf{R})$, which leaves the effective Lagrangian invariant, and the general formula is found to be [8]

$$
\begin{pmatrix} a_{2D} \\ a_2 \\ a_{1D} \\ a_1 \end{pmatrix} \rightarrow \begin{pmatrix} \alpha a_{2D} + \beta a_2 + p a_1 \\ \gamma a_{2D} + \delta a_2 + q a_1 \\ a_{1D} + p(\gamma a_{2D} + \delta a_2) - q(\alpha a_{2D} + \beta a_2) - pq a_1 \\ a_1 \end{pmatrix}, \tag{12}
$$

where $\begin{pmatrix} \alpha & \beta \\ \gamma & \delta \end{pmatrix} \in SL(2, \mathbf{Z})$ and $p, q \in \mathbf{Q}$. Note that this monodromy transformation for the combination (a_{2D}, a_2, a_1) is exactly the same as that for SQCD with massive quark hypermultiplets, if we regard a_1 as the same mass of the hypermultiplets such that $m = \sqrt{2}a_1$. This fact means that the $U(1)$ gauge interaction part plays the only role as the mass term for the $SU(2)$ gauge dynamics. This observation is consistent with our assumption. On the other hand, the $SU(2)$ dynamics plays an important role for the $U(1)$ gauge interaction part, as can be seen in the transformation law of a_{1D}. This monodromy transformation is also used to derive dual variables associated with the BPS states. As a result, the prepotential of our theory turns out to be essentially the same as the result in [3] with understanding the relation $A_1 = m/\sqrt{2}$,

$$
F(A_2, A_1, \Lambda_{N_f}, \Lambda_L) = F^{(SW)}_{SU(2)}(A_2, m, \Lambda_{N_f})\Big|_{A_1 = \frac{m}{\sqrt{2}}} + C A_1^2, \tag{13}
$$

where the first term is the prepotential of $\mathcal{N} = 2$ SQCD with hypermultiplets having the same mass m, and C is free parameter. The freedom of the parameter C is used to determine the scale of the Landau pole relative to the scale of the $SU(2)$ dynamics.

B. Effective Potential

The effective potential can be read off from the above Lagrangian with the FI term such that [3]

$$
V = b_{11}|F_1|^2 + b_{12}(F_1 F_2^\dagger + F_1^\dagger F_2) + b_{22}|F_2|^2 + \frac{1}{2}b_{11}D_1^2 + b_{12}D_1 D_2 + \frac{1}{2}b_{22}D_2^2
$$

---

[3] We suppose that the potential is described by the adequate variables associated with the light BPS states. For instance, the variable a_2 is understood implicitly as $-a_{2D}$, when we consider the effective potential for the monopole.

$$+ (D_2 + nD_1)(|M|^2 - |\tilde{M}|^2) + |F_M|^2 + |F_{\tilde{M}}|^2 \tag{14}$$
$$+ \sqrt{2}(F_2 M\tilde{M} + a_2 M F_{\tilde{M}} + a_2 \tilde{M} F_M + h.c.)$$
$$+ \sqrt{2}(nF_1 M\tilde{M} + na_1 M F_{\tilde{M}} + na_1 \tilde{M} F_M + h.c.) + \xi D_1 ,$$

where $F_I(I = 1, 2, M, \tilde{M})$ denotes the auxiliary field of the corresponding chiral multiplet, $D_J(J = 1, 2)$ denotes the auxiliary field of the corresponding vectormultiplet V_J, and the effective gauge coupling is defined as $b_{ij} = (1/4\pi)\text{Im}\tau_{ij}$. Eliminating these auxiliary fields by using their equations of motion,

$$D_1 = \frac{1}{\det b}\left\{(b_{12} - nb_{22})(|M|^2 - |\tilde{M}|^2) - \xi b_{22}\right\},$$
$$D_2 = \frac{1}{\det b}\left\{-(b_{11} - nb_{12})(|M|^2 - |\tilde{M}|^2) + \xi b_{12}\right\},$$
$$F_1 = \frac{\sqrt{2}}{\det b}(b_{12} - nb_{22})(M\tilde{M})^\dagger, \tag{15}$$
$$F_2 = \frac{\sqrt{2}}{\det b}(nb_{12} - b_{11})(M\tilde{M})^\dagger,$$
$$F_M = -\sqrt{2}(a_2^\dagger + na_1^\dagger)\tilde{M}^\dagger,$$
$$F_{\tilde{M}} = -\sqrt{2}(a_2^\dagger + na_1^\dagger)M^\dagger,$$

where $\det b = b_{22}b_{11} - b_{12}^2$, we obtain

$$V = \frac{b_{22}}{2\det b}\xi^2 + S(a_2, a_1)\left\{(|M|^2 - |\tilde{M}|^2)^2 + 4|M\tilde{M}|^2\right\}$$
$$+ 2T(a_2, a_1)(|M|^2 + |\tilde{M}|^2) - U(a_2, a_1)(|M|^2 - |\tilde{M}|^2), \tag{16}$$

where S, T and U are defined as

$$S(a_2, a_1) = \frac{1}{2b_{22}} + \frac{(b_{12} - nb_{22})^2}{2b_{22}\det b}, \tag{17}$$
$$T(a_2, a_1) = |a_2 + na_1|^2, \tag{18}$$
$$U(a_2, a_1) = \frac{b_{12} - nb_{22}}{\det b}\xi. \tag{19}$$

The stationary conditions with respect to the hypermultiplets,

$$\frac{\partial V}{\partial M^\dagger} = M\left\{2S(|M|^2 - |\tilde{M}|^2) + 2T - U\right\} + 4S\tilde{M}^\dagger(M\tilde{M}) = 0, \tag{20}$$
$$\frac{\partial V}{\partial \tilde{M}^\dagger} = \tilde{M}\left\{-2S(|M|^2 - |\tilde{M}|^2) + 2T + U\right\} + 4SM^\dagger(M\tilde{M}) = 0, \tag{21}$$

lead to three solutions as follows:

$$1.\ M = \tilde{M} = 0;\ \ V = \frac{b_{22}}{2\det b}\xi^2, \tag{22}$$
$$2.\ |M|^2 = -\frac{2T - U}{2S},\ \ \tilde{M} = 0;\ \ V = \frac{b_{22}}{2\det b}\xi^2 - S|M|^4. \tag{23}$$
$$3.\ M = 0,\ |\tilde{M}|^2 = -\frac{2T + U}{2S};\ \ V = \frac{b_{22}}{2\det b}\xi^2 - S|\tilde{M}|^4. \tag{24}$$

The solution Eq. (23) or Eq. (24), in which the light hypermultiplet acquires the vacuum expectation value, is energetically favored, because of $\det b > 0$ and $S(a_2, a_1) > 0$. Since the hypermultiplet appears in the theory as the light BPS state around the singular point on moduli space, the potential minimum is expected to emerge there. On the other hand, the solution Eq. (22) describes the potential energy away from the singular points, which smoothly connects with the solution Eq. (23) or Eq. (24).

C. Periods and Effective Couplings

It was shown that the effective potential is described by the periods a_{2D}, a_2 and the effective gauge coupling b_{ij}. In this subsection, we derive the periods and the effective gauge couplings in order to give an explicit description of the effective potential. As already discussed, the periods are the same as that of SQCD, which were derived in both cases with the massless [13–16] and the massive [8,17–19] hypermultiplets. There are some different descriptions of the periods with such as the Weierstrass functions [8], the hypergeometric functions [17], the modular functions [18] and the elliptic integrals [19]. In our analysis, we use the integral representation. On the other hand, the effective coupling τ_{ij} is described in terms of the Weierstrass functions.

We first review how to obtain the periods a_{2D} and a_2. The elliptic curves of $\mathcal{N} = 2$ SQCD with hypermultiplets having the same mass m were found to be [3]

$$y^2 = x^2(x - u) + P_{N_f}(x, u, m, \Lambda_{N_f}),\tag{25}$$

where the polynomials $P_{N_f}(N_f = 1, 2)$ are given by

$$P_1 = \frac{\Lambda_1^3}{4}mx - \frac{\Lambda_1^6}{64},\tag{26}$$

$$P_2 = -\frac{\Lambda_2^4}{64}(x - u) + \frac{\Lambda_2^2}{4}m^2x - \frac{\Lambda_2^4}{32}m^2.\tag{27}$$

In this case, the mass formula of the BPS state with the quantum number $(n_e, n_m)_n$ is given by $M_{BPS} = \sqrt{2}|n_m a_{2D} + n_e a_2 + nm/\sqrt{2}|$. If λ is a meromorphic differential on the curve Eq. (25) such that

$$\frac{\partial \lambda}{\partial u} = \frac{\sqrt{2}}{8\pi}\frac{dx}{y},\tag{28}$$

the periods are given by the contour integrals

$$a_{2D} = \oint_{\alpha_1} \lambda, \ a_2 = \oint_{\alpha_2} \lambda,\tag{29}$$

where the cycles α_1 and α_2 are defined so as to encircle e_2 and e_3, and e_1 and e_3, respectively (see. Fig. 1). Meromorphic differentials are given by

$$\lambda_{SW}^{(N_f=1)} = -\frac{\sqrt{2}}{4\pi}\frac{ydx}{x^2} = \frac{\sqrt{2}}{4\pi}\left[-\frac{dx}{2y}\left(3x - 2u + \frac{m\Lambda_1^3}{4x}\right) + dx\frac{d}{dx}\left(\frac{x}{y}\right)\right],\tag{30}$$

$$\lambda_{SW}^{(N_f=2)} = -\frac{\sqrt{2}}{4\pi}\frac{ydx}{x^2 - \frac{\Lambda^4}{64}} = -\frac{\sqrt{2}}{4\pi}\frac{dx}{y}\left[x - u + \frac{m^2\Lambda_2^2}{4\left(x + \frac{\Lambda^2}{8}\right)}\right].\tag{31}$$

8

Each differential have the single pole at $x = 0$ for $N_f = 1$ and $x = -\frac{\Lambda_2}{8}$ for $N_f = 2$. For both cases, the residue is given by

$$\text{Res}\lambda_{SW}^{(N_f)} = \frac{1}{2\pi i}(-1)\frac{m}{\sqrt{2}}. \tag{32}$$

We calculate the periods by using the Weierstrass normal form for later convenience. In this form, the algebraic curve is rewritten by new variables $x = 4X + \frac{u}{3}$ and $y = 4Y$, such that

$$Y^2 = 4X^3 - g_2^{(N_f)}X - g_3^{(N_f)} = 4(X - e_1)(X - e_2)(X - e_3), \tag{33}$$
$$\sum_{i=1}^{3} e_i = 0,$$

where $g_2^{(N_f)}$ and $g_3^{(N_f)}$ are explicitly written by

$$g_2^{(1)} = \frac{1}{4}\left(\frac{u^2}{3} - \frac{m\Lambda_1^3}{3}\right), \tag{34}$$

$$g_3^{(1)} = \frac{1}{16}\left(-\frac{mu\Lambda_1^3}{12} + \frac{\Lambda_1^6}{64} + \frac{2u^3}{27}\right), \tag{35}$$

$$g_2^{(2)} = \frac{1}{16}\left(\frac{4}{3}u^2 + \frac{\Lambda_2^4}{16} - m^2\Lambda_2^2\right), \tag{36}$$

$$g_3^{(2)} = \frac{1}{16}\left(\frac{m^2\Lambda_2^4}{32} - \frac{u}{12}m^2\Lambda_2^2 - \frac{u\Lambda_2^4}{96} + \frac{2u^3}{27}\right). \tag{37}$$

Converting the Seiberg-Witten differentials of Eqs.(30) and (31) into the Weierstrass normal form and substituting them into Eq.(29), we obtain the integral representations of the periods as follows (a_{2D} and a_2 are denoted by a_{21} and a_{22}, respectively):

$$a_{2i}^{(N_f=1)} = -\frac{\sqrt{2}}{4\pi}\left(-uI_1^{(i)} + 12I_2^{(i)} + \frac{m\Lambda_1^3}{16}I_3^{(i)}(c)\right), \tag{38}$$

$$a_{2i}^{(N_f=2)} = -\frac{\sqrt{2}}{4\pi}\left(-\frac{4}{3}uI_1^{(i)} + 8I_2^{(i)} + \frac{m^2\Lambda_2^2}{8}I_3^{(i)}(c)\right), \tag{39}$$

where c is the pole of the differentials, and $c = -\frac{u}{12}$ for $N_f = 1$ and $c = -\frac{u}{12} - \frac{\Lambda_2^2}{32}$ for $N_f = 2$. Integrals $I_1^{(i)}, I_2^{(i)}$ and $I_3^{(i)}$ are defined as

$$I_1^{(i)} = \frac{1}{2}\oint_{\alpha_i}\frac{dX}{Y}, \quad I_2^{(i)} = \frac{1}{2}\oint_{\alpha_i}\frac{XdX}{Y}, \quad I_3^{(i)}(c) = \frac{1}{2}\oint_{\alpha_i}\frac{dX}{Y(X-c)}. \tag{40}$$

The roots e_i of the polynomial defining the cubic are chosen so as to lead to the correct asymptotic behavior for large $|u|$,

$$a_{2D}^{(N_f)}(u) \sim i\frac{4-N_f}{2\pi}\sqrt{2u}\log\frac{u}{\Lambda_{N_f}^2}, \quad a_2^{(N_f)}(u) \sim \frac{\sqrt{2u}}{2}. \tag{41}$$

9

A correct choice is the following:

$N_f = 1$ case:
$$e_1 = \frac{1}{48} \frac{-24\Lambda_1^3 m + 32u^2 + 2^{1/3} H(u,m,\Lambda_1)^{2/3}}{H(u,m,\Lambda_1)^{1/3}},$$

$$e_2 = \frac{1}{96} \frac{8(1-3i)(3\Lambda_1^2 m - 4u^2) - 2^{1/3} i(-i+\sqrt{3}) H(u,m,\Lambda_1)^{2/3}}{2^{2/3} H(u,m,\Lambda_1)^{1/3}},$$

$$e_3 = \frac{1}{96} \frac{8(1+3i)(3\Lambda_1^2 m - 4u^2) + 2^{1/3} i(i+\sqrt{3}) H(u,m,\Lambda_1)^{2/3}}{2^{2/3} H(u,m,\Lambda_1)^{1/3}}, \tag{42}$$

$$H(u,m,\Lambda_1) = 27\Lambda_1^6 + 128u^3$$
$$+ 3\Lambda_1^3(-48mu + \sqrt{3}\sqrt{27\Lambda_1^6 - 256(m^2-u)u^2 + 32\Lambda_1^3(8m^3 - 9mu)}),$$

$N_f = 2$ case:
$$e_1 = \frac{u}{24} - \frac{\Lambda_2^2}{64} - \frac{1}{8}\sqrt{u + \frac{\Lambda_2^2}{8} + \Lambda_2 m}\sqrt{u + \frac{\Lambda_2^2}{8} - \Lambda_2 m},$$

$$e_2 = \frac{u}{24} - \frac{\Lambda_2^2}{64} + \frac{1}{8}\sqrt{u + \frac{\Lambda_2^2}{8} + \Lambda_2 m}\sqrt{u + \frac{\Lambda_2^2}{8} - \Lambda_2 m}, \tag{43}$$

$$e_3 = -\frac{u}{12} + \frac{\Lambda_2^2}{32}.$$

Fixing the contours of the cycles relative to the positions of the poles, which is equivalent to fix the $U(1)$ charges (baryon numbers) for the BPS states, the final formulae are given by

$$a_{2i}^{(N_f=1)} = -\frac{\sqrt{2}}{4\pi}\left(-uI_1^{(i)} + 12I_2^{(i)} + \frac{m\Lambda_1^3}{16}I_3^{(i)}\left(-\frac{u}{12}\right)\right) - \frac{m}{\sqrt{2}}\delta_{i2}, \tag{44}$$

$$a_{2i}^{(N_f=2)} = -\frac{\sqrt{2}}{4\pi}\left(-\frac{4}{3}uI_1^{(i)} + 8I_2^{(i)} + \frac{m^2\Lambda_2^2}{8}I_3^{(i)}\left(-\frac{u}{12} - \frac{\Lambda_2^2}{32}\right)\right) - \frac{m}{\sqrt{2}}\delta_{i2}, \tag{45}$$

with the integral $I_i^{(1)}$ $(i=1,2)$ explicitly given by

$$I_1^{(1)} = \int_{e_2}^{e_3} \frac{dX}{Y} = \frac{iK(k')}{\sqrt{e_2 - e_1}}, \tag{46}$$

$$I_2^{(1)} = \int_{e_2}^{e_3} \frac{XdX}{Y} = \frac{ie_1}{\sqrt{e_2 - e_1}}K(k') + i\sqrt{e_2 - e_1}E(k'), \tag{47}$$

$$I_3^{(1)} = \int_{e_2}^{e_3} \frac{dX}{Y(X-c)} = \frac{-i}{(e_2-e_1)^{3/2}}\left\{\frac{1}{k+\tilde{c}}K(k') + \frac{4k}{1+k}\frac{1}{\tilde{c}^2 - k^2}\Pi_1\left(\nu, \frac{1-k}{1+k}\right)\right\}, \tag{48}$$

where $k^2 = \frac{e_3 - e_1}{e_2 - e_1}$, $k'^2 = 1 - k^2 = \frac{e_2 - e_3}{e_2 - e_1}$, $\tilde{c} = \frac{c - e_1}{e_2 - e_1}$, and $\nu = -\left(\frac{k+\tilde{c}}{k-\tilde{c}}\right)^2\left(\frac{1-k}{1+k}\right)^2$. The formulae for $I_i^{(2)}$ are obtained from $I_i^{(1)}$ by exchanging the roots, e_1 and e_2. In Eqs. (46)-(48), K, E, and Π_1 are the complete elliptic integrals [20] given in Appendix A.

Next let us consider the effective coupling defined as Eq. (10). The effective couplings τ_{22} and $\tau_{12}(=\tau_{21})$ are obtained by

10

$$\tau_{22} = \frac{\partial a_{2D}}{\partial a_2} = \frac{\omega_1}{\omega_2}, \tag{49}$$

$$\tau_{12} = \left.\frac{\partial a_{2D}}{\partial a_1}\right|_{a_2} = \left.\frac{\partial a_{2D}}{\partial a_1}\right|_u - \tau_{22}\left.\frac{\partial a_2}{\partial a_1}\right|_u = -\frac{2z_0}{\omega_2}, \tag{50}$$

where ω_i is the period of the Abelian differential,

$$\omega_i = \oint_{\alpha_i} \frac{dX}{Y} = 2I_1^{(i)} \quad (i = 1, 2), \tag{51}$$

and z_0 is defined as

$$z_0 = -\frac{1}{\sqrt{e_2 - e_1}} F(\phi, k); \quad \sin^2\phi = \frac{e_2 - e_1}{c - e_1} . \tag{52}$$

Here $F(\phi, k)$ is the incomplete elliptic integral of the first kind given in Appendix B. The effective coupling τ_{11} is described in terms of the Weierstrass function. First consider the period a_{1D} by using the Riemann bilinear relation [21],

$$\oint_{\alpha_1} \phi \oint_{\alpha_2} \omega - \oint_{\alpha_1} \omega \oint_{\alpha_2} \phi = 2\pi i \sum_{n=1}^{N_p} \mathrm{Res}_{x_n^+}\phi \int_{x_n^-}^{x_n^+} \omega, \tag{53}$$

where ϕ and ω are meromorphic and holomorphic differentials, respectively, N_p is the number of poles ($N_p = 1$ in our case), and $x_n^\pm$ are poles of ϕ on the positive and negative Riemann sheets. Substituting $\phi = \partial\lambda_{SW}^{(N_f)}/\partial a_1$ and $\omega = \partial\lambda_{SW}^{(N_f)}/\partial a_2$ into Eq. (53), we obtain (see Fig. 2 for the definition of the contour)

$$a_{1D}^{(N_f)} = -\sum_{n=1}^{N_p} \int_{x_n^-}^{x_n^+} \lambda_{SW} + \tilde{C} , \tag{54}$$

where $\tilde{C}$ is a constant independent of a_2. The effective coupling τ_{11} is obtained by differentiating Eq. (54) with respect to a_1 with a_2 fixed. This integral can be evaluated by the uniformization method discussed in Appendix B. After regularizing the integral by using the freedom of the constant $\tilde{C}$, we finally obtain (see also Appendix B for details)

$$\tau_{11} = -\frac{1}{\pi i}\left[\log\sigma(2z_0) + \frac{4z_0^2}{\omega_2}I_1^{(2)}\right] + C, \tag{55}$$

where σ is the Weierstrass sigma function, and C is the constant in Eq. (13).

Note that, since the gauge coupling b_{11} is found to be a monotonically decreasing function of large $|a_1|$ with fixed u, and vice versa (see, for example, Fig. 3 in the case of fixed a_1), the scale of the Landau pole is defined as $|a_1| = \Lambda_L$ at which $b_{11} = 0$. The large Λ_L required by our assumption is realized by taking an appropriate value for C. In the following analysis, we fix $C = 4\pi i$, which corresponds to $\Lambda_L \sim 10^{17-18}$ for fixed $\Lambda_{N_f} \sim O(1)$

In $N_f = 1$ case, we plot the effective couplings b_{ij} along real u-axis in Fig. 3. Here, the dynamical scale is normalized as $\Lambda_1 = (256/27)^{1/6}$, and the parameter $a_1 = \sqrt{2}$ is fixed. As expected, in the figure of b_{22}, there are three singular points: the dyon point ($u \sim -2.6$), the

11

monopole point ($u \sim 2.4$) and the quark singular point ($u \sim 4.2$). While the existence of the quark singular point is understood based on the perturbative discussion, the appearance of the dyon and the monopole singular points is the result from the $SU(2)$ dynamics. Note that, in addition to the quark singular point, there appear two singular points in the figures of b_{12} and b_{11}. This result means that the $SU(2)$ dynamics plays an important role for the $U(1)$ gauge interaction part in the infrared region on the moduli space, as pointed out in the subsection A.

IV. POTENTIAL ANALYSIS

Based on the results given by the previous sections, let us now investigate the vacuum structure of our theory. Since the effective potential is the function of two complex moduli parameters u and a_1, it is a very complicated problem to figure out behaviors of the effective potential in the whole parameter space. However, note that, for our aim it is enough to evaluate the potential energy just around the singular points, since these points are energetically favored (see Eqs. (22)-(24)). The singular points on the moduli space parameterized by u flow according to the variation of a_1. In the following discussion, we evaluate the effective potential along the flow of the singular points, and examine which point is energetically favored on the line of the flow.

A. Vacuum Structure in $N_f = 1$ case

Here we analyze the vacuum structure of our theory in $N_f = 1$ case. Let us first discuss the flow of the singular points. In the following analysis, the dynamical scale is fixed as $\Lambda_1 = (256/27)^{1/6}$. The singular points on the u-plane are given by the solutions of the cubic polynomial [3],

$$\Delta = \frac{\Lambda_1^6}{16} \left[-u^3 + m^2 u^2 + \frac{9}{8} \Lambda_1^3 m u - \Lambda_1^3 m^3 - \frac{27}{256} \Lambda_1^6 \right] \bigg|_{a_1 = \frac{m}{\sqrt{2}}} = 0. \tag{56}$$

For simplicity, we consider the case $\mathrm{Im}\, a_1 = 0$ in the following. The flow of the singular points is sketched in Fig. 4. For $a_1 = 0$, there are three singular points at $u_1 = -1$, $u_2 = \exp(i\pi/3)$ and $u_3 = \exp(-i\pi/3)$, respectively. These singular points correspond to the appearance of the BPS states with quantum numbers $(n_e, n_m) = (2, 1)$, $(1, 1)$ and $(0, 1)$, respectively. In this case, there is non-anomalous $\mathbf{Z}_3$ symmetry on the moduli space. The $(2, 1)_1$ dyon point is moving to the left on real u-axis, as a_1 is increasing. The $(1, 1)_1$ dyon point and the $(0, 1)_0$ monopole point are moving to the right and approaching real u-axis, and eventually collide on real u-axis for $a_1 = \frac{3}{4\sqrt{2}} \Lambda_1$. This collision point is called Argyres-Douglas (AD) point [22], at which the two collapsing states are simultaneously massless, and the theory is believed to transform into the superconformal theory. After the collision and for $a_1 > \frac{3}{4\sqrt{2}} \Lambda_1$, quantum numbers of two BPS states, $(n_m, n_e)_n = (1, 1)_1$ and $(0, 1)_0$, change into $(1, 0)_1$ and $(0, 1)_0$, respectively, due to the conjugation of monodromy [19]. As a_1 is increasing further, both of the singular points, u_2 and u_3, are moving to the right on real u-axis (u_2 approaches the infinity faster than u_3). On the other hand, as a_1 is decreasing from $a_1 = 0$, the dyon point

u_1 is moving to the right on real u axis. The dyon point u_2 and the monopole point u_3 are approaching imaginary u-axis to the infinities, $u_2 \to +i\infty$ and $u_3 \to -i\infty$, respectively.

Before analyzing the vacuum structure, let us see the dependence of the effective potential on the SUSY breaking parameter ξ. For $a_1 = 0$, the effective potential around the dyon singular point u_1 is depicted in Fig. 5. with various values of ξ. In the left figure, the top figure with the cusp and the bottom figure show the effective potential without and with the dyon condensation, respectively. Note that the cusp is smoothed out in the effective potential including the dyon condensation. This fact means that the dyon really enjoys the correct degrees of freedom in the effective theory around the singular point. We can see that values of the potential minimum and the width of the dyon condensation are controlled by the scale of ξ, as expected.

Now we investigate the vacuum structure by varying the values of a_1. In the following analysis, the SUSY breaking parameter is fixed as $\xi = 0.1$. First, let us see the evolution of the potential energy along the flow of the $(2,1)_1$ dyon point (u_1). The effective potentials for $a_1 = 1/8$, 0 and $-1/8$ from left to right are depicted in Fig. 6. We can check that the potential minimum appears on the singular point for fixed a_1. The right figure shows the evolution of the potential energy along the flow of the singular point. We can find that, as a_1 is decreasing, the potential energy is monotonically decreasing. Therefore, the effective potential is not bounded from below along the flow of the $(2,1)_1$ dyon point.

Next we investigate the effective potential around the other two singular points. For $a_1 < \frac{3}{4\sqrt{2}}\Lambda_1$, the effective potential has the CP symmetry, and is invariant under the transformation $u \leftrightarrow u^\dagger$. Hence, the potential energies on these points are degenerate. As a_1 is increasing, the potential energy is monotonically decreasing toward the AD point $(a_1 = \frac{3}{4\sqrt{2}}\Lambda_1)$, at which two singular points collide. For $a_1 > \frac{3}{4\sqrt{2}}\Lambda_1$, two singular points appear again, the $(0,1)_0$ monopole point and the $(1,0)_1$ quark singular point. The effective potential for various values of $a_1 > \frac{3}{4\sqrt{2}}\Lambda_1$ is depicted in Fig. 7. For $a_1 > \frac{3}{4\sqrt{2}}\Lambda_1$, all the singular points are on real u-axis. From the left figure, we see that there appears the potential minimum only on the quark singular point (the left minimum corresponds to the minimum around $(2,1)_1$ dyon point already depicted in Fig. 6). The $(0,1)_0$ monopole condensation is too small for the effective potential to have its minimum on the monopole point. Since, as a_1 is increasing further, the potential energy on the quark singular point is monotonically decreasing as depicted in the right figure, we find that the effective potential is not bounded from below along the flow of this singular point. [4]

In the case Im$a_1 = 0$, the evolutions of the potential energies along the flows of the singular points are simultaneously sketched in Fig. 8. The effective potential is found to be the runaway type, and is monotonically decreasing toward the boundary of the defined region of moduli space. We can analyze the effective potential for general complex values of a_1, and find that the same results come out. In conclusion, there is neither well-defined vacuum nor local minimum in the effective theory.

----

[4] To be correct, there is a possibility that the local minimum may exist near the AD point. However, our description of the effective theory is not applicable around the point, since the condensations of two BPS states are well overlapped. For detailed discussions in this situation, see the next subsection B.

B. Vacuum Structure in $N_f = 2$ case

Next, we analyze the vacuum structure for $N_f = 2$ case. Again, let us first consider the flow of the singular points. In the following analysis, the dynamical scale is fixed as $\Lambda_2 = 2\sqrt{2}$. In $N_f = 2$ case, the discriminant of the algebraic curve can be easily solved such that

$$u_1 = -m\Lambda_2 - \frac{\Lambda_2^2}{8}\bigg|_{a_1 = \frac{m}{\sqrt{2}}}, \quad u_2 = m\Lambda_2 - \frac{\Lambda_2^2}{8}\bigg|_{a_1 = \frac{m}{\sqrt{2}}}, \quad u_3 = m^2 + \frac{\Lambda_2^2}{8}\bigg|_{a_1 = \frac{m}{\sqrt{2}}}. \tag{57}$$

We investigate the case $\text{Im}\,a_1 = 0$, for simplicity. The flow of the singular points is sketched in Fig. 9. For $a_1 = 0$, the singular points appear at $u_1 = u_2 = -1$ and $u_3 = 1$. Here, at $u = -1$, two singular points degenerate. For non-zero $a_1 > 0$, [5] this singular point splits into two singular points u_1 and u_2, which correspond to the BPS states with quantum numbers $(1,1)_{-1}$ and $(1,1)_1$, respectively. As a_1 is increasing, these singular points, u_1 and u_2, are moving to the left and the right on real u-axis, respectively. Two singular points, u_2 and u_3, collide and degenerate at the AD point ($u = \frac{3\Lambda_2^2}{8}$) for $a_1 = \frac{\Lambda_2}{2\sqrt{2}}$. As a_1 is increasing further, there appear two singular points u_2 and u_3 again, and quantum numbers of the corresponding BPS states, $(1,1)_1$ and $(0,1)_0$, change into $(1,0)_1$ and $(1,-1)_1$, respectively. The singular point u_2 is moving to the right faster than u_3.

We investigate the vacuum structure by varying the values of a_1. For $0 < a_1 < \frac{\Lambda_2}{2\sqrt{2}}$, the effective potential is plotted in Fig. 10. While there appear the potential minima at two singular points u_1 and u_2, the monopole condensation is too small for the potential to have a minimum at the singular point u_3. The top and bottom figures in the middle show the effective potential without and with the dyon condensations, respectively. The cusps are smoothed out in the bottom figure, as in the case $N_f = 1$. The evolutions of the potential energies on the singular points u_2 and u_3 are depicted in Fig. 11. We find that both of them are decreasing toward the point $a_1 = 0$, and thus the effective potential is bounded from below, at least, along real u-axis.

Next, we examine whether the effective potential is bounded in all the directions for general complex a_1 values. As an example, let us consider the case $\text{Re}\,a_1 = 0$. For $a_1 \neq 0$, the two singular points u_1 and u_2 appear on the imaginary u-axis with $\text{Re}\,u = -1$. The effective potential is depicted in Fig. 12 along this axis for $a_1 = i\frac{\sqrt{2}}{4}$. There appear two potential minima at the singular points. The right figure shows the evolution of the potential energy along the flow of the singular point u_1, [6] and we find that the effective potential is also bounded in this direction. We can check that the effective potential is bounded from below for all the values of small $|a_1|$. Therefore, the effective potential seems to have the local minimum at the points $u = -1$ and $a_1 = 0$.

---

[5] We consider only the case $a_1 > 0$, since the result for $a_1 < 0$ can be obtained by exchanging $u_1 \leftrightarrow u_2$, as be seen from the first two equations in Eq. (57).

[6] Two potential minima for fixed a_1 are degenerate, since the effective potential has the CP symmetry under the exchange $u \leftrightarrow u^\dagger$ in the case $\text{Re}\,a_1 = 0$.

However, note that our description is not applicable for small $|a_1|$, since the condensations of two dyon states are going to overlap with each other (see Fig. 10). Unfortunately, we have no knowledge about the correct description of the effective theory in this situation. Nevertheless, we conclude that there must appear the local minimum with broken SUSY in the limit $a_1 \to 0$ from the result in the following. In this limit, the effective potential without the dyon condensations is depicted in Fig. 13. We can find that there appears the potential minimum at $u = -1$, and the value of the effective potential on the cusp is non-zero, $V \sim 0.0061 > 0$. If we had the correct description of the effective theory for $a_1{=}0$, this cusp might be smoothed out. However, there is no reason that SUSY is restored at $u = -1$, because the correct effective theory must have no singularity for the Kahler metric. Therefore, there is the promising possibility of the appearance of the local minimum with broken SUSY at $u = -1$ and $a_1 = 0$.

Finally, let us get back to the case $\text{Im}a_1 = 0$. For $a_1 > \frac{\Lambda_2}{2\sqrt{2}}$, the effective potential has two minima only at two singular points u_1 and u_2. The monopole condensation is too small for the effective potential to have a minimum at u_3. The plot of the effective potential is similar to Fig. 7. While the evolution of the potential energy along the singular point u_1 is the same as for $0 < a_1 < \frac{\Lambda_2}{2\sqrt{2}}$, the potential energy on the quark singular point u_2 is monotonically decreasing, as a_1 is increasing. Thus, there is a runaway direction along the flow of the quark singular point. We can find the same global structure along the flow of the quark singular point for general complex a_1 values.

The evolutions of the potential energies along the flows of the singular points are simultaneously sketched in Fig. 14. The global structure of the effective potential is the same as in the case $N_f = 1$, namely, the runaway type. However, we find the promising possibility that there exists the local minimum with broken SUSY in the theory. Since there is no well-defined vacuum on the runaway direction, this minimum with broken SUSY is the unique and promising candidate for the vacuum in the theory. Unfortunately, we have no knowledge of the correct description about the effective theory around the degenerate dyon point.

V. CONCLUSION

We analyzed the vacuum structure of spontaneously broken $\mathcal{N} = 2$ SUSY gauge theory with the Fayet-Iliopoulos term. Our theory is based on the gauge group $SU(2) \times U(1)$ with $N_f = 1, 2$ massless quark hypermultiplets having the same $U(1)$ charges. The $U(1)$ gauge interaction was necessary introduced to include the Fayet-Iliopoulos term in the theory. It was shown that there are degenerate vacua in the classical potential even in the absence of SUSY. This degeneracy is expected to be smoothed out, once quantum corrections are taken into account. Then, we investigated the effective potential, and analyzed the the vacuum structure of the theory.

The effective action was formulated up to the leading order for the SUSY breaking parameter ξ. In our framework, the $U(1)$ gauge interaction part was treated as the cut-off theory under the assumption that the $U(1)$ gauge interaction has no effect on the $SU(2)$ gauge dynamics. Thus, the moduli space in the theory was restricted within the region smaller than the cut-off scale, the Landau pole. Considering the monodromy transformation,

we found that the prepotential consistent with the assumption was the same as the one in SQCD with massive quark hypermultiplets.

The effective potential was the function of the moduli parameters. Examining the minimum of the effective potential, we found that the singular points on the moduli space were energetically favored, because of the condensations of the light BPS states. The singular points on the u-plane flowed according to the values of the moduli parameter a_1. Thus, we analyzed the effective potential along the flows of the singular points, and examined which point was energetically favored on the line of the flow.

In $N_f = 1$ case, the effective potential was found to be the runaway type and monotonically decreasing toward the ultraviolet region in the moduli space. We observed that there was neither well-defined vacuum nor the local minimum in this case. In $N_f = 2$ case, there was also the runaway direction along the flow of the quark singular point, and the global structure was the same as in $N_f = 1$ case. However, we found the promising possibility that the local minimum with broken SUSY appears at the degenerate dyon point. Therefore, this point is the promising candidate for the well-defined vacuum. Unfortunately, we have no knowledge about the correct description of the effective theory around the degenerate singular point, since the condensations of two BPS states well overlap there.

The difference of our result from that in SQED is worth noticing. In SQED, the potential minimum appears at the massless singular point, and SUSY is formally restored there, because of the singularity of the Kahler metric. On the other hand, in our case with $N_f = 2$ hypermultiplets, we found that the value of the potential minimum was non-zero, and thus SUSY was really broken there (at least in analysis of the effective potential without the dyon condensations). This result means that the singularity of the Kahler metric is removed by the effect of the $SU(2)$ gauge dynamics in the infrared region on the moduli space.

Finally we comment on the possibility that the theory has the global minimum. Note that the behavior of the effective potential changes according to the number of flavors N_f, since both of the periods and the effective couplings depend on N_f. Indeed, we observed that the structures of the effective potentials were different in two cases $N_f = 1, 2$. If we consider the extended version of our theory with $N_f = 3, 4$ quark hypermultiplets, we may find the global minimum in the theory. Although this extension makes our analysis much more complicated and difficult, it will be interesting.

APPENDIX A:

In this appendix, we demonstrate the derivations of the integrals $I_i^{(j)}$ in Eqs. (46)-(48). The complete elliptic integrals are given as follows.

$$K(k) = \int_0^1 \frac{dx}{[(1 - x^2)(1 - k^2 x^2)]^{1/2}}, \tag{A1}$$

16

$$E(k) = \int_0^1 dx \left(\frac{1 - k^2 x^2}{1 - x^2} \right)^{1/2},$$

$$\Pi_1(\nu, k) = \int_0^1 \frac{dx}{[(1 - x^2)(1 - k^2 x^2)]^{1/2}(1 + \nu x^2)}.$$

The integrals $I_i^{(j)}$ are described in terms of the above complete elliptic integrals through some steps of changing variables in the integrations.

First, demonstrate the derivation of Eq. (46).

$$
\begin{aligned}
I_1^{(1)} &= \int_{e_2}^{e_3} \frac{dX}{Y} \\
&= \int_{e_2}^{e_3} \frac{dX}{\sqrt{4(X - e_1)(X - e_2)(X - e_3)}} \\
&= \frac{i}{2\sqrt{e_2 - e_1}} \int_0^{k'^2} \frac{dt}{[t(t - 1)(t - k'^2)]^{1/2}},
\end{aligned}
\tag{A2}
$$

where we changed the variable X by $t = -\frac{X - e_2}{e_2 - e_1}$. Further, changing the variable t by $t = 1 + k + \frac{1}{\zeta - \frac{1}{2k}}$ and rescaling ζ as $x = 2k\frac{1+k}{1-k}\zeta$, we obtain

$$I_1^{(1)} = \frac{i}{\sqrt{e_2 - e_1}} \frac{2}{1 + k} K\left(\frac{1 - k}{1 + k} \right). \tag{A3}$$

Using the relation

$$\frac{2}{1 + k} K\left(\frac{1 - k}{1 + k} \right) = K(k'), \tag{A4}$$

we obtain Eq. (46). Repeating the same steps for the integral $I_2^{(1)}$, we obtain

$$
\begin{aligned}
I_2^{(1)} &= \int_{e_2}^{e_3} \frac{X dX}{Y} \\
&= \frac{i}{\sqrt{e_2 - e_1}} \frac{2}{1 + k} \left[\{e_2 - (e_2 - e_1)(1 + k)\} K\left(\frac{1 - k}{1 + k} \right) \right. \\
&\quad \left. + 2k(e_2 - e_1)\Pi_1\left(-\left(\frac{1 - k}{1 + k} \right)^2, \frac{1 - k}{1 + k} \right) \right].
\end{aligned}
\tag{A5}
$$

Using Eq. (A4) and the following relations,

$$(1 - \bar{k}^2)\Pi(-\bar{k}^2, \bar{k}) = E(\bar{k}), \ (1 + k)E\left(\frac{1 - k}{1 + k} \right) = E(k') + kK(k'), \tag{A6}$$

where $\bar{k} = \frac{1-k}{1+k}$, we obtain Eq. (47). Finally, for $I_3^{(1)}$, the same steps lead to

$$I_3^{(1)}(c) = \int_{e_2}^{e_3} \frac{dX}{Y(X-c)}$$

$$= \frac{-i}{(e_2-e_1)^{\frac{3}{2}}} \frac{1}{\tilde{c}+k} \frac{1}{1+k}$$

$$\times \int_{-1}^{1} \frac{dx}{\left[\left(1 - \left(\frac{1-k}{1+k}\right)^2 x^2\right)(1-x^2)\right]^{\frac{1}{2}}} \left[1 - \frac{2k}{\tilde{c}+k} \frac{1}{\frac{1-k}{1+k}x - \frac{\tilde{c}-k}{\tilde{c}+k}}\right], \tag{A7}$$

where $\tilde{c} = \frac{c-e_1}{e_2-e_1}$. Using the relations Eq. (A4), we obtain Eq. (48).

APPENDIX B:

In this subsection, we show the derivations of the effective couplings in term of the Weierstrass functions. It is convenient to introduce the uniformization variable z through the map with the Weierstrass $\wp$ function,

$$(\wp(z), \wp'(z)) = (X, Y). \tag{B1}$$

Using this map, the half period $\omega_i/2$ is mapped into the root $e_i = \wp(\omega_i/2)$ $(\omega_3 = \omega_1 + \omega_2)$. The inverse map is defined as

$$z = \Psi^{-1}(x_0) = \int_{x_0}^{\infty} \frac{dX}{Y} = -\frac{1}{\sqrt{e_2-e_1}} F(\phi, k), \tag{B2}$$

where we changed the integration variable X by $t^2 = (e_2 - e_1)/(X - e_1)$, and $F(\phi, k)$ is the incomplete elliptic integral given by

$$F(\phi, k) = \int_0^{\sin\phi} \frac{dt}{[(1-t^2)(1-k^2t^2)]^{1/2}}; \quad \sin^2\phi = \frac{e_2-e_1}{x_0-e_1}. \tag{B3}$$

We derive the effective couplings, τ_{12} and τ_{11}, by using the map of Eq. (B1). The effective coupling τ_{12} is described by

$$\tau_{12} = \left.\frac{\partial a_{2D}}{\partial a_1}\right|_{a_2} = \left.\frac{\partial a_{2D}}{\partial a_1}\right|_u - \tau_{22}\left.\frac{\partial a_2}{\partial a_1}\right|_u. \tag{B4}$$

The partial derivative of the periods a_{2D} and a_2 with respect to a_1 can be calculated by using Eqs. (29)-(31) as

$$\left.\frac{\partial a_{2i}}{\partial a_1}\right|_u = \oint_{\alpha_i} \left.\frac{\partial \lambda_{SW}}{\partial a_1}\right|_u = Q^{(N_f)}(a_1, \Lambda_{N_f}) \int_{e_j}^{e_3} \frac{dX}{2Y(X-c)} \quad (i \neq j), \tag{B5}$$

where the coefficient $Q^{(N_f)}$ is given by

$$Q^{(N_f)}(a_1, \Lambda_{N_f}) = -\frac{N_f(\sqrt{2}a_1)^{N_f-1}\Lambda_{N_f}^{4-N_f}}{16\pi}. \tag{B6}$$

Using the map of Eq. (B1), the integral can be described as

18

$$\left. \frac{\partial a_{2i}}{\partial a_1} \right|_u = Q^{(N_f)} \int_{\omega_j}^{\omega_3} \frac{dz}{2(\wp(z) - \wp(z_0))}$$

$$= \frac{Q^{(N_f)}}{2} \frac{1}{\wp'(z_0)} \left(\log \frac{\sigma(z - z_0)}{\sigma(z + z_0)} + 2z\zeta(z_0) \right), \tag{B7}$$

where $\wp(z_0) = c$, $\zeta(z)$ is the Weierstrass zeta function, and we used the definition of the Weierstrass sigma function, $\zeta(z) = \frac{d}{dz} \log \sigma(z)$, and the relation

$$\frac{\wp'(z_0)}{\wp(z) - \wp(z_0)} = \zeta(z - z_0) - \zeta(z + z_0) + 2\zeta(z_0). \tag{B8}$$

Taking into account that Y corresponds to $\wp'(z)$ under the map of Eq. (B1), the pole $\wp'(z_0)$ can be easily obtained as

$$\wp'(z_0)^2 = -\left(\frac{N_f 2^{(N_f-1)/2} \Lambda_{N_f}^{4-N_f}}{32} \right)^2. \tag{B9}$$

Using the pseudo periodicity of the Weierstrass sigma function,

$$\sigma(z_0 + \omega_i) = -\sigma(z_0) \exp\left(2\zeta\left(\frac{\omega_i}{2}\right)\left(z_0 + \frac{1}{2}\omega_i\right) \right), \tag{B10}$$

we obtain

$$\left. \frac{\partial a_{2i}}{\partial a_1} \right|_u = -\frac{1}{\pi i} \left[\omega_i \zeta(z_0) - 2z_0 \zeta\left(\frac{\omega_i}{2}\right) \right]. \tag{B11}$$

The zeta function at half period can be described by the integral representations such as

$$\zeta\left(\frac{\omega_i}{2}\right) = -I_2^{(i)}. \tag{B12}$$

Substituting Eq. (B11) into Eq. (B4) and using the Legendre relation

$$\omega_1 \zeta\left(\frac{\omega_2}{2}\right) - \omega_2 \zeta\left(\frac{\omega_1}{2}\right) = i\pi, \tag{B13}$$

we finally obtain

$$\tau_{12} = -\frac{2z_0}{\omega_2}. \tag{B14}$$

Next we derive the effective coupling τ_{11}, which is given by differentiating a_{1D} of Eq. (54) with respect to a_1 with a_2 fixed such as

$$\tau_{11} = -\int_{x_n^-}^{x_n^+} \left[\left. \frac{\partial \lambda_{SW}}{\partial u} \right|_{a_1} \left. \frac{\partial u}{\partial a_1} \right|_{a_2} + \left. \frac{\partial \lambda_{SW}}{\partial a_1} \right|_u \right] + \frac{\partial \tilde{C}}{\partial a_1}. \tag{B15}$$

The integral can be evaluated by using the map (B1). Although the integral contains divergence, it can be regularized by using the freedom of the integration constant $\tilde{C}$. Let us demonstrate this regularization by introducing the regularization parameter ϵ as follows.

$$\tau_{11} = -\int_{x_0^- + \epsilon}^{x_0^+ + \epsilon} \left[\frac{\partial \lambda_{SW}}{\partial u} \bigg|_{a_1} \left(-\frac{\partial u}{\partial a_2} \bigg|_{a_1} \frac{\partial a_2}{\partial a_1} \bigg|_{a_2} \right) + \frac{\partial \lambda_{SW}}{\partial a_1} \bigg|_u \right] + \frac{\partial \tilde{C}}{\partial a_1}$$

$$= -\int_{-z_0 + \epsilon}^{z_0 + \epsilon} dz \left[-\frac{1}{\pi i \omega_2} \left(\omega_2 \zeta(z_0) - 2z_0 \zeta\left(\frac{\omega_2}{2}\right) \right) + \frac{Q^{(N_f)}}{4(\wp(z) - \wp(z_0))} \right] + \frac{\partial \tilde{C}}{\partial a_1}$$

$$= -\frac{1}{\pi i} \left(\log \sigma(2z_0) - \frac{4z_0^2}{\omega_2} \zeta\left(\frac{\omega_2}{2}\right) \right) + \frac{1}{\pi} \log \sigma(\epsilon) + \frac{1}{2} + \frac{\partial \tilde{C}}{\partial a_1}. \tag{B16}$$

The divergence part, $\log \sigma(\epsilon)$, can be subtracted by taking the integration constant such that $\tilde{C} = Ca_1 - \frac{a_1}{2} - \frac{a_1}{\pi} \log \sigma(\epsilon)$, and we finally obtain Eq. (55) with the relation of Eq. (B12).

REFERENCES

[1] N. Seiberg, Phys. Lett. B 318, 469 (1993); N. Seiberg, Phys. Rev. D 49, 6857 (1994); K. Intriligator, R.G. Leigh and N. Seiberg, Phys .Rev. D 50, 1092 (1994).

[2] N. Seiberg and E. Witten, Nucl. Phys. B 426, 19 (1994).

[3] N. Seiberg and E. Witten, Nucl. Phys. B 431, 484 (1994).

[4] O. Aharony, J. Sonnenshein, M.E. Peskin and S. Yankielowicz, Phys. Rev. D 52, 6157 (1995).

[5] N. Evans, S.D.H. Hsu and M. Schwetz, Phys. Lett. B 355, 475 (1995); N. Evans, S.D.H. Hsu and M. Schwetz, Nucl. Phys. B 456, 205 (1995).

[6] L. Alvarez-Gaume, J. Distler, C. Kounnas and M. Marino, Int. J. Mod. Phys. A 11, 4745 (1996).

[7] L. Alvarez-Gaume and M. Marino, Int. J. Mod. Phys. A 12, 975 (1997).

[8] L. Alvarez-Gaume, M. Marino and F. Zamora, Int. J. Mod. Phys. A 13, 403 (1998); ibid 13, 1847 (1998).

[9] N. Arkani-Hamed and R. Rattazzi, Phys.Lett. B 454, 290 (1999); M.A. Luty and R. Rattazzi, JHEP 11, 001 (1999).

[10] P. Fayet, Nucl. Phys. B 113, 135 (1976).

[11] M. Arai and N. Kitazawa, Proceeding of JINR Workshop "Supersymmetry and Quantum symmetry" (2000) 169; hep-th/9904214.

[12] V.A. Miransky, Phys. Lett. 91B, 421 (1980); P.I. Fomin, V.P. Gusynin, V.A. Miransky and Yu. A. Sitenko, Riv. Nuov. Cim. 6, 1 (1983); V.A. Miransky, Nuov. Cim. 90A, 149 (1985).

[13] A. Klemm, W. Lerche, S. Theisen and S. Yankielowicz, Int. J. Mod. Phys. A 11, 1929 (1996).

[14] K. Ito and S.-K. Yang, Phys. Lett. B 366, 165 (1996).

[15] A. Bilal and F. Ferrari, Nucl. Phys. B 480, 589 (1996).

[16] J. M. Isidro, A. Mukherjee, J. P. Nunes and H. J. Schnitzer, Nucl. Phys. B 492, 647 (1997).

[17] T. Masuda and H. Suzuki, Int. J. Mod. Phys. A 12, 3413 (1997).

[18] A. Brandhuber and S. Stieberger, Int. J. Mod. Phys. A13, 1329 (1998).

[19] A. Bilal and F. Ferrari, Nucl. Phys. B 516, 175 (1998).

[20] A. Erdelyi et al., *Higher Transcendental Functions*, Vol. 1, McGraw-Hill, New york (1953).

[21] P. Griffiths and J. Harris, *Principles of Algebraic geometry*, New York, John Wiley (1978).

[22] P. C. Argyres and M. R. Douglas, Nucl. Phys. B 448, 93 (1995); P.C. Argyres, R. Plesser, N. Seiberg and E. Witten, Nucl. Phys. B 461, 71 (1996).
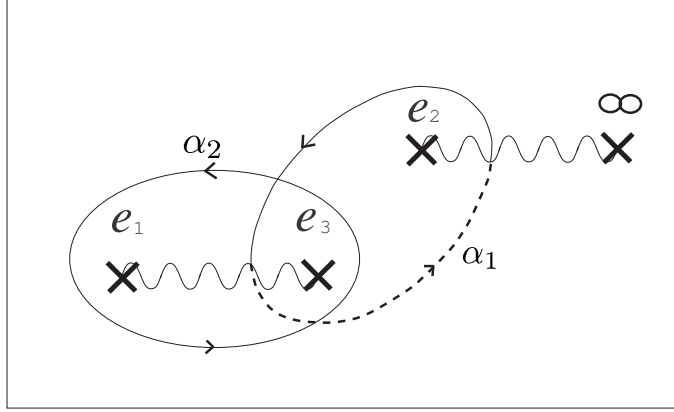
FIGURES

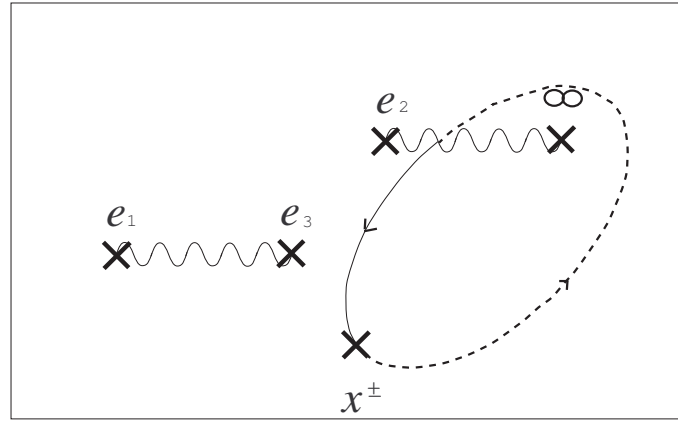
FIG. 1.   The contours α_1 and α_2.

FIG. 2.   The contour of the integral Eq. (53).
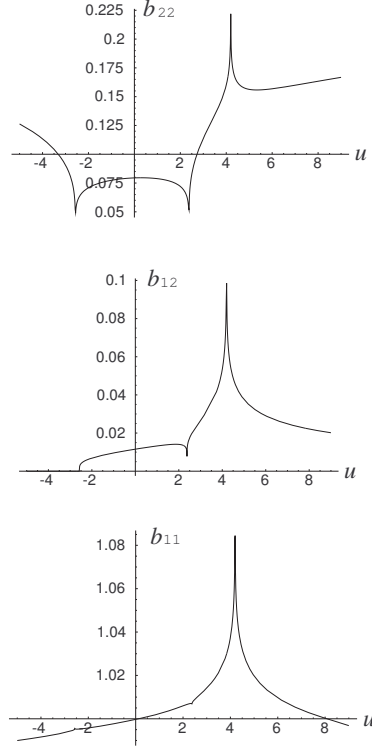
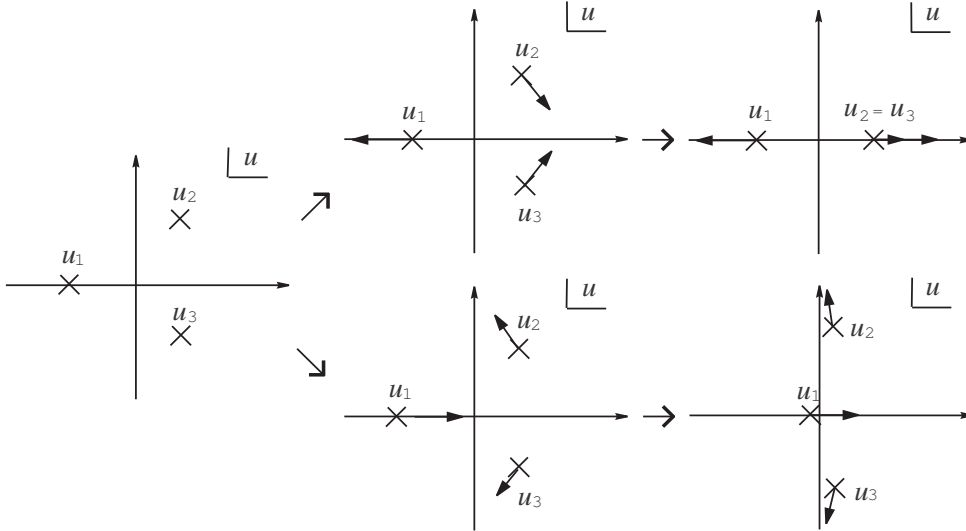FIG. 3. The effective gauge couplings b_{ij} for $a_1 = \sqrt{2}$ along real u-axis.

FIG. 4. The flow of the singular points on u-plane for fixed a_1 in the case $\mathrm{Im}\,a_1 = 0$. The left figure shows the positions of the singular points for $a_1 = 0$, the upper figures shows the evolutions of the singular points for $a_1 > 0$, and the lower figures show them as $a_1 < 0$ is decreasing.
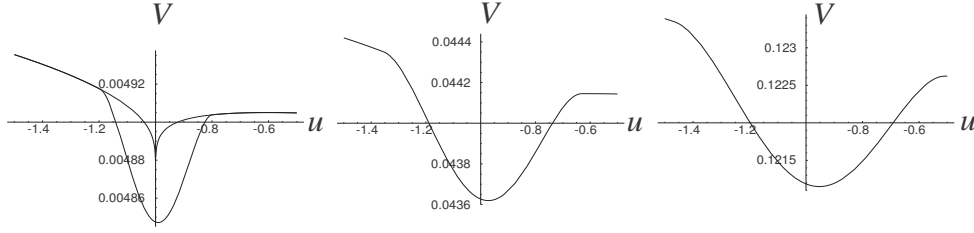
FIG. 5.   The effective potential around the $(2,1)_1$ dyon point for $a_1 = 0$ and $\xi = 0.1$, 0.3, 0.5 (from left to right) along real u-axis.
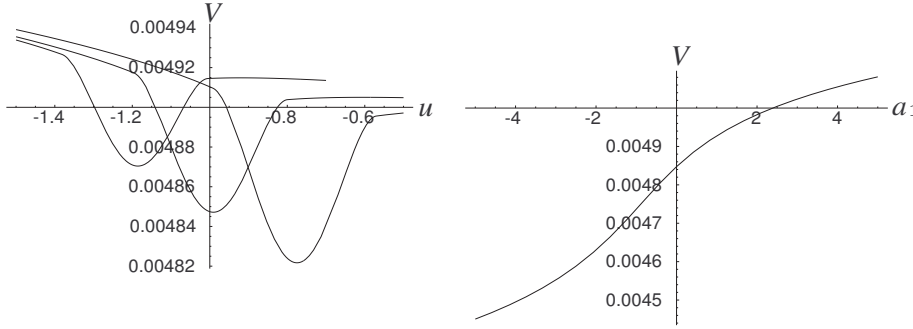
FIG. 6.   The left figure shows the effective potential for $a_1 = 1/8$ (left), 0 (middle), $-1/8$ (right). The right figure shows the evolution of the potential energy along the flow of the $(2,1)_1$ dyon point.
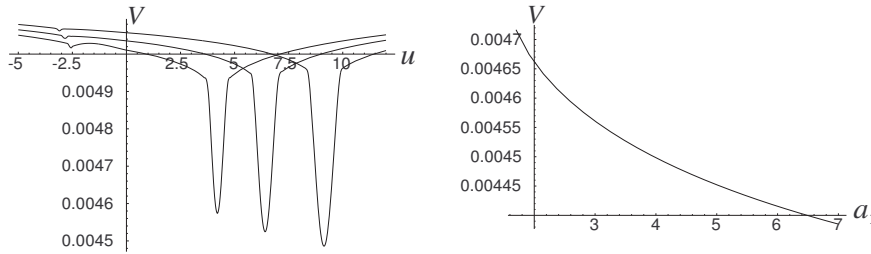
FIG. 7.   The left figure shows the effective potential along real u-axis for $a_1 = \frac{2}{\sqrt{2}}$ (left), $\frac{2.5}{\sqrt{2}}$ (middle) and $\frac{3}{\sqrt{2}}$ (right). The right figure shows the evolution of the potential energy along the flow of the quark singular point.
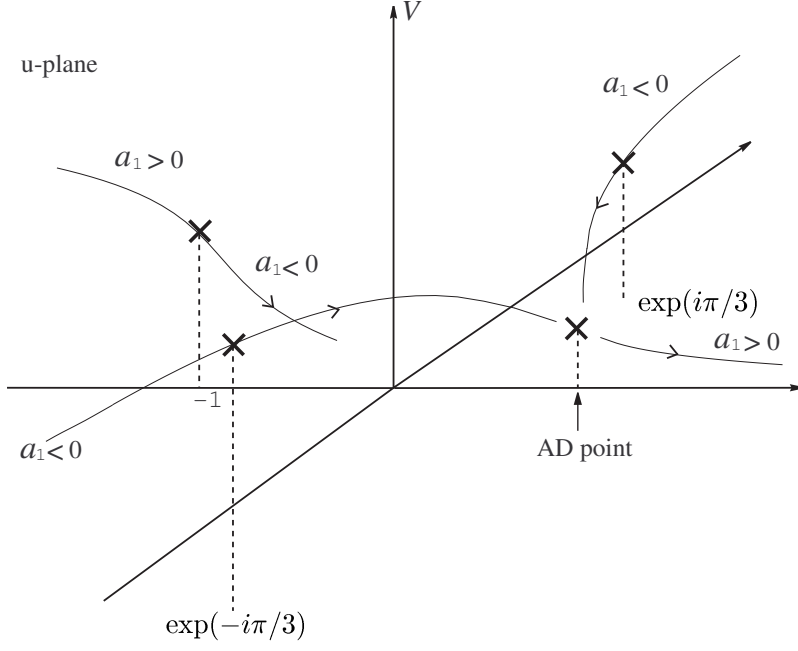
FIG. 8.   The evolutions of the potential energies along the flows of the singular points.
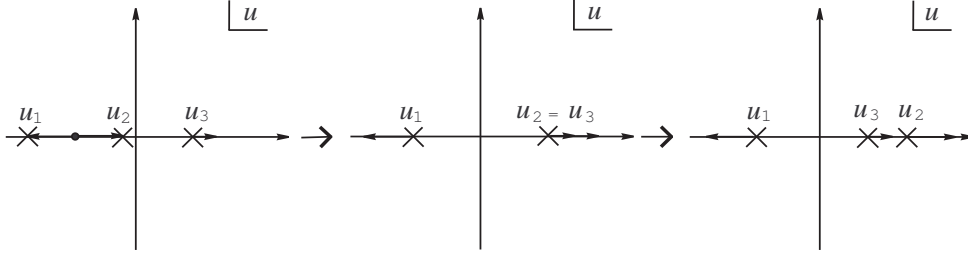
FIG. 9.   The flow of the singular points in the case $\mathrm{Im}\, a_1 = 0$. The figures show the position of the singular points for $a_1 = 0$, $a_1 = \frac{\Lambda_2}{2\sqrt{2}}$ and $a_1 > \frac{\Lambda_2}{2\sqrt{2}}$ from left to right.
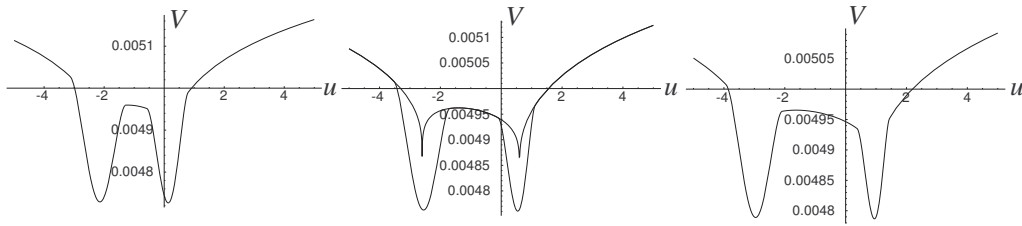

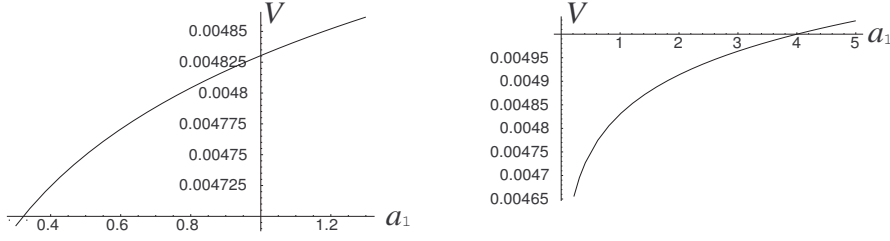FIG. 10.   The effective potential for $a_1 = 0.3$ (left), $a_1 = 0.4$ (middle) and $a_1 = 0.5$ (right).

25

FIG. 11. The evolutions of the potential energies along the flows of the $(1,1)_{-1}$ dyon point (left) and the $(1,1)_1$ dyon point (right).
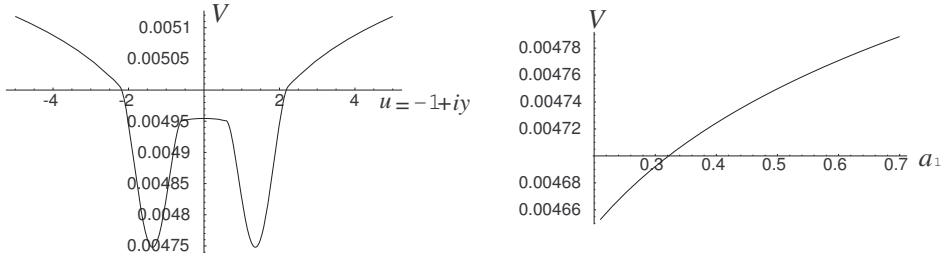

FIG. 12. The effective potential (left) for $a_1 = i\frac{\sqrt{2}}{4}$ along imaginary u-axis with $\mathrm{Re}\,u = -1$, and the evolution of the potential energy (right) along the flow of the singular point u_1 in the case $\mathrm{Re}\,a_1 = 0$.
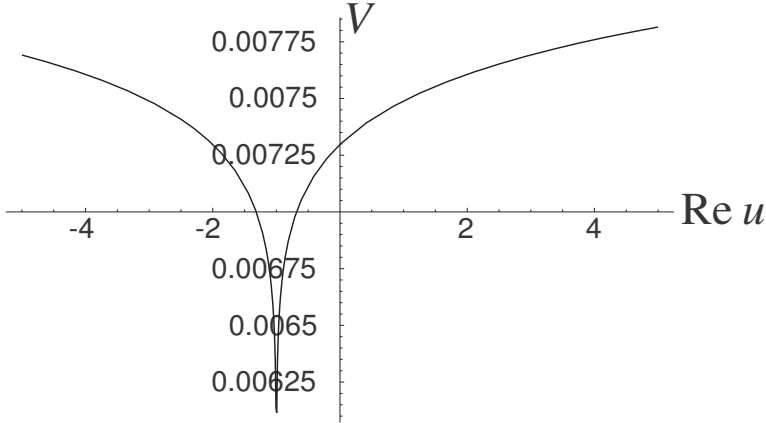

FIG. 13. The effective potential without the contribution of the dyon condensations in the limit $a_1 \to 0$.
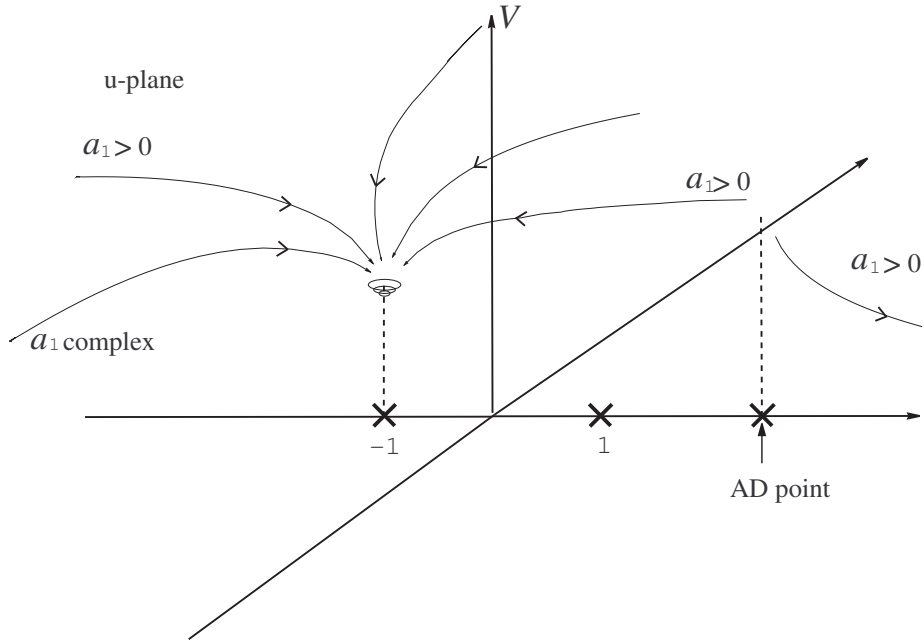
FIG. 14. The evolutions of the potential energies along the flows of the singular points.